Anion photoelectron spectroscopy of C_5H^-

Sean M. Sheehan,[1] Bradley F. Parsons,[1,a)] Terry A. Yen,[1] Michael R. Furlanetto,[1,b)] and Daniel M. Neumark[1,2,c)]
[1]*Department of Chemistry, University of California, Berkeley, Berkeley, California 94720-1460, USA*
[2]*Chemical Sciences Division, Lawrence Berkeley National Laboratory, Berkeley, California 94720, USA*

(Received 29 February 2008; accepted 27 March 2008; published online 1 May 2008)

Anion photoelectron spectroscopy is performed on the C_5H^- species. Analogous to C_3H^- and C_3D^-, photodetachment transitions are observed from multiple, energetically close-lying isomers of the anion. A linear and a cyclic structure are found to have electron binding energies of 2.421 ± 0.019 eV and 2.857 ± 0.028 eV, respectively. A cyclic excited state is also found to be 1.136 eV above the linear $^2\Pi$ C_5H ground state. Based on our assignments of the observed transitions and previous calculations on the energetics of neutral C_5H isomers, the cyclic $^1A_1$ anion state is found to lie 0.163 eV below the ^3A linear anion. © *2008 American Institute of Physics*. [DOI: 10.1063/1.2912056]

I. INTRODUCTION

The C_5H radical is believed to be an important intermediate in the reaction pathway to the formation of larger carbon containing molecules in molecular clouds and interstellar envelopes and to the formation of larger polycyclic aromatic hydrocarbons in combustion processes. Recent crossed molecular beam studies have shown that C_5H is formed in its linear $^2\Pi$ ground state through a single collision processes with acetylene,[1]

$$C_3 + C_2H_2 \rightarrow C_5H(\tilde{X}\,^2\Pi) + H. \quad (1)$$

Equation (1) represents an example of a class of reactions, $C_p + C_nH_m \rightarrow C_{n+p}H_{m-1} + H$, thought to account for the formation of molecules with large carbon chain backbones detected in the interstellar medium.[2,3] Due to the high abundance of $C(^3P)$[4,5] and acetylene[6] detected in interstellar clouds, the smallest of these reactions ($p=1$, $n=m=2$) is thought to be most important, followed by reactions of acetylene with larger bare carbon chains. Bare carbon chains up to C_5, carbon monohydride chains up to C_8H, and the negatively charged monohydrides C_4H^-, C_6H^-, and C_8H^- have been discovered in space.[7–11] In this paper, we report photoelectron spectra of C_5H^- in order to characterize the energetics and structure of both C_5H and C_5H^-.

Most of the carbon chain species found in space have been linear owing to their large dipole moments and amenability to detection via radiotelescope. The linear form of C_5H was identified in the laboratory and in space by its microwave spectrum in 1986.[12,13] Since then the linear isomer has been theoretically[14–18] and experimentally studied.[19,20] Most of the theoretical work has focused on the ground $^2\Pi$ state, but Haubrich *et al.*[17] have computed the electronic spectra of the linear isomer using multireference configuration interaction methods. In the more recent experiments, McCarthy and Thaddeus[19] studied the hyperfine couplings of the linear ^{13}C substituted chains, while Ding *et al.*[20] identified the $A\,^2\Delta \leftarrow X\,^2\Pi$, $B\,^2\Sigma^- \leftarrow X\,^2\Pi$, and $C\,^2\Sigma^+ \leftarrow X\,^2\Pi$ electronic transitions, all involving a $\sigma \rightarrow \pi$ electronic excitation.

The C_3H radical is now known to exist in cyclic and linear forms, as the anion does.[21–26] The laboratory and astrophysical detection[22] of cyclic C_3H has motivated several theoretical[16,17,27] and experimental[27–29] studies aimed at identifying other nonlinear isomers of the larger C_nH chains. For even n, a single resonance structure of the linear chain with alternating acetylenic bonds dominates the energy landscape. Only linear isomers of both the anions and neutrals of the even series with $n<8$ have been experimentally seen.[20,30–34] For odd n, there is no dominant resonance structure, and multiple close lying isomers may result.

Crawford *et al.*[16] employed high level coupled-cluster calculations on the C_5H neutral potential energy surface and found six other stable isomers ranging from 0.2 to 3 eV above the linear $^2\Pi$ ground state. One of these isomers, a cyclic C_5H isomer with a three-carbon ring (Fig. 2, structure II), was unambiguously identified by Apponi *et al.*[29] via Fourier-transform microwave spectroscopy. Haubrich *et al.*[17] calculated vertical excitation energies to excited states of several neutral isomers. Bowie and co-workers[27,28,35] have theoretically investigated the anion, finding four low-lying isomers at the B3LYP level of theory. The linear anion is a triplet in its lowest energy state, followed closely by a singlet state only 0.13 eV higher in energy. Although the linear species was found to be the ground state in the neutral, $C_2CHC_2^-$ was found to be the anion ground state, lying 0.15 eV below the linear isomer. Experiments by Bowie and Blanksby *et al.*[27] based on mass spectrometry showed evidence for this form of the anion and the corresponding neutral.

Our laboratory has investigated several C_nH radicals by anion photoelectron spectroscopy and related techniques.[33,34,36] These results have yielded electron affinities (EAs) and excited state energies in the radicals. Our

[a)]Permanent address: Department of Chemistry, Creighton University, Omaha, NE 68178, USA.
[b)]Permanent address: Physics Division, Los Alamos National Laboratory, MS H803, P.O. Box 1663, Los Alamos, NM 87545, USA.
[c)]Author to whom correspondence may be addressed. Electronic mail: dneumark@berkeley.edu.

recent study[26] of C_3H^- was particularly instructive as we were able to determine which close-lying photodetachment transitions originated from either cyclic or linear C_3H^-. Here, we present anion photoelectron spectra of C_5H^- at photodetachment wavelengths of 355 nm (3.495 eV), 299 nm (4.115 eV), and 266 nm (4.661 eV). We find evidence for photodetachment from both linear and cyclic anion isomers to the corresponding lowest lying neutral states as well as to an excited state of the cyclic isomer. In the next section, we give the details of our experiment, while Sec. III gives the results of our experiments and electronic structure calculations. Section IV provides assignments of our spectra using previous experimental data, calculations, and Franck–Condon (FC) simulations.

II. EXPERIMENTAL

The photoelectron spectrometer has been described elsewhere[37,38] and only details relevant to the current experiment are given. C_5H^- is formed by expanding propyne ($H_3C—C\equiv CH$) seeded in N_2 through a pulsed valve (Parker-Hannefin), followed by a high voltage discharge. The mixture consisted of 8% propyne and 1% CO_2 in a balance of N_2. The gas pulse expands supersonically from the nozzle through the orifices of a set of annular discharge plates pulsed to 900–950 V. The throat of the discharge is intersected by a 1 keV electron beam for stability of ion production. The pulsed beam passes through a skimmer, after which anions are extracted into a linear reflectron time-of-flight (TOF) mass spectrometer with a mass resolution ($m/\Delta m$) of 2000.[39] Ion optics steer and focus the ion packets toward the interaction region, where they are intersected by the detachment laser. Detached electrons are detected and their flight times recorded using a chevron-mounted dual microchannel plate detector at the end of an ~1 m long, magnetically shielded flight tube perpendicular to both the molecular and laser beam axes.

The electron kinetic energy (eKE) is related to the electron time-of-flight (TOF) by the following equation:

$$e\mathrm{KE} = \frac{1}{2}m_e\left(v_{\mathrm{ion}}^2 + \frac{l^2}{\mathrm{TOF}^2}\right), \tag{2}$$

where m_e is the electron mass, v_{ion} is the velocity of the parent ion, and l is the length between the laser interaction region and the electron detector. Under the best resolution, the full width half maxima of an electron peak in kinetic energy space (ΔE) has been found to be 8 meV at 0.65 eKE. From Eq. (1), it can shown that $\Delta E \sim e\mathrm{KE}^{3/2}$ and the resolution of a given electron peak ($e\mathrm{KE}/\Delta E$) will be lower with increasing eKE.

For this experiment, the third (355 nm, 3.495 eV) and fourth (266 nm, 4.661 eV) harmonics of a Nd:YAG (neodynium:yttrium aluminum garnet) laser, as well as the first Stokes line of 266 nm from a 325 psig H_2 Raman cell (299 nm, 4.115 eV) were used. The laser polarization angle (θ), the angle between the electric field vector of the laser and the direction of electron collection, was set to either 0° or 90° in order to obtain angular information of the photoelectrons. The angular distribution of the photoelectrons is given by[40]

$$\frac{d\sigma}{d\Omega} = \frac{\sigma_{\mathrm{tot}}}{4\pi}\left[1 + \frac{\beta}{2}(3\cos^2\theta - 1)\right], \tag{3}$$

where σ_{tot} is the total photodetachment cross section, and β is the anisotropy parameter which varies from −1 to 2. Each feature in the PE spectrum has a characteristic β calculated from the spectra using the equation,

$$\beta = \frac{I_{0^\circ} - I_{90^\circ}}{\frac{1}{2}I_{0^\circ} + I_{90^\circ}}, \tag{4}$$

where I_{0° and I_{90° are the intensities of the peak taken at θ=0° and 90°. Anisotropy parameters can be useful as a probe of vibronic coupling and as a means of distinguishing close-lying neutral←anion electronic transitions.[33]

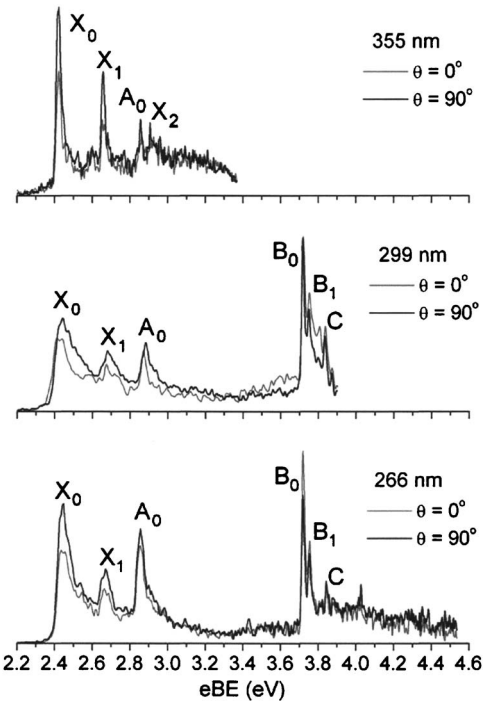

FIG. 1. TOF photoelectron spectra of C_5H^- at 355 nm (top), 299 nm (middle), and 266 nm (bottom) plotted in electron binding energy (eBE). Black and gray traces are taken at laser polarization angles of 90° and 0°, respectively.

III. RESULTS

A. Photoelectron spectra

Figure 1 shows the photoelectron spectra of C_5H^- at 355 nm (3.495 eV, top), 299 nm (4.115 eV, middle), and 266 nm (4.661 eV, bottom). Peak positions and anisotropy parameters for the largest peaks are given in Table I. The spectra show signal versus electron binding energy (eBE) from 2.2 to 4.6 eV. The eBE scale is obtained from the eKE using $e\mathrm{BE}=h\nu - e\mathrm{KE}$, where $h\nu$ is the photon energy. No features were observed below 2.2 eV. Spectra were collected over 200 000 laser shots at laser polarization angles of 0° (gray trace) and 90° (black trace) for each wavelength. Elec-

TABLE I. Peak positions in eV, anisotropy parameters, and vibrational and electronic assignments. Anisotropy parameters were only measured for peaks with appreciable intensity or resolution in both the 355 and 266 nm spectra.

Peak	Energy (eV)	$\beta_{355\ nm}$	$\beta_{299\ nm}$	$\beta_{266\ nm}$		Assignment
X_0	2.421	−0.3	−0.2	−0.2	0_0^0	$^2\Pi \leftarrow {}^3A$ (isomer I)
X_1	2.658	−0.2	−0.2	−0.2	3_0^1	
X_2	2.908	⋯	⋯	⋯	3_0^2	
A_0	2.857	⋯	−0.1	−0.1	0_0^0	$^2B_2 \leftarrow {}^1A_1$ (isomer II)
B_0	3.720	⋯	0.0	0.2	0_0^0	$^2A_1 \leftarrow {}^1A_1$ (isomer II)
B_1	3.755	⋯	0.1	0.1	5_0^1	
C	3.8–3.9	⋯	⋯	⋯	⋯	$^4\Sigma^- \leftarrow {}^3A$ (isomer I)

tron intensities versus *e*BE at the two polarizations were scaled according to the raw electron intensities recorded as a function of TOF.

The 355 nm spectra show four large peaks, X_0, X_1, A_0, and X_2, superimposed upon a broad quasicontinuous signal extending from 2.4 to 3.4 eV. The broad feature is not from the background photoelectrons, the production of which is minimal at 355 nm, and is apparently from photodetachment of C_5H^-. Peaks X_0, X_1, and X_2 are evenly spaced with an average spacing of 0.244 eV (1964 cm^{-1}) and appear to be a vibrational progression with peak X_0 as the vibrational origin. The nature of peak A_0 is more complex, as discussed below. The major peaks in the spectra all have slightly negative anisotropy parameters, as shown in Table I.

At both 299 and 266 nm, the major peaks seen at 355 nm are still apparent but with lower resolution due to the increased *e*KE. In addition, two prominent new peaks appear around 3.7 eV, labeled B_0 and B_1, and several smaller features from 3.8 to 4.0 eV, which are collectively labeled *C*. Peaks B_0 and B_1 have slightly positive anisotropy parameters. The most interesting point of comparison between the spectra at different wavelengths is that the relative intensity of peak A_0 is substantially higher in both the 299 and 266 nm spectra than at 355 nm. A_0 appears to have a markedly different *e*KE dependence than band *X*, with much lower intensities closer to threshold. This evidence suggests that A_0 is not a transition to a vibrational level of the same electronic state responsible for the rest of the 355 nm spectrum, and instead most likely originates from a different electronic transition or structural isomer.

B. Electronic structure calculations

Electronic structure calculations were performed on the relevant neutral and anionic isomers of C_5H, as determined by previous studies. Several calculations have already been carried out on the anion[18,27] and the neutral.[15–18] The current calculations serve to reproduce the representative force constants for each state in order to generate FC factors for the purpose of simulating and interpreting the photoelectron spectra. Our calculations were carried out with density functional theory (DFT) using the Becke three-parameter Lee, Yang, Parr exchange-correlation functional[41,42] (B3LYP) along with the correlation consistent polarized valence double-ζ basis set (cc-pVDZ).[43] All computations were performed using the GAUSSIAN03 program.[44]

Crawford *et al.*[16] performed coupled-cluster [CCSD and CCSD(T)] and equation-of-motion coupled cluster (EOMEA, EOMIP-CCSD) calculations with DZP and TZ2P basis sets and found seven minima on the neutral potential energy surface. Of these seven structures, Blanksby *et al.*[27] found four to be stable on the anion potential energy surface. They performed B3LYP calculations with an aug-cc-pVDZ basis set for geometry optimization and RCCSD(T) calculations to find more accurate energies at potential energy minima. Only these four isomers, whose structures are shown in Fig. 2, are of interest in the current study. In the present study, B3LYP calculations were undertaken on the geometries, vibrational frequencies, and energetics of the ground states of the anion and neutral for each of the four isomers. In addition, neutral excited states of isomers I and II were also calculated. Table II shows the current B3LYP calculated bond lengths, bond angles, and dihedral angles corresponding to the labels in Fig. 2, along with the previous calculations and experiment for comparison. No previous calculations for comparison are given for the anion states since our B3LYP calculations essentially reproduce the struc-

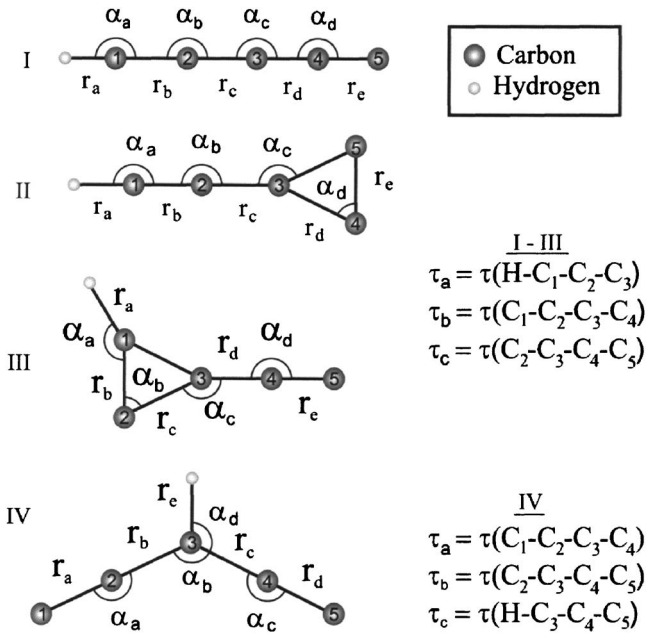

FIG. 2. Approximate geometries of the isomers relevant to the current work. Bond lengths (r), angles (α), and dihedrals (τ) correspond to the values given in Table II.

TABLE II. Geometries from current and previous calculations and experiment.

		State	Method	Sym.	r_a	r_b	r_c	r_d	r_e	α_a	α_b	α_c	α_d	τ_a	τ_b	τ_c
I	Anion	^3A	B3LYP/cc-pVDZ[a]	C_1	1.078	1.272	1.312	1.316	1.296	150.5	174.3	174.8	178.4	173.5	−52.4	162.0
	Neutral	$^2\Pi$	B3LYP/cc-pVDZ[a]	$C_{\infty v}$	1.074	1.234	1.331	1.277	1.318							
		$^2\Pi$	EOMEA-CCSD/TZ2P[b]	$C_{\infty v}$	1.061	1.216	1.346	1.256	1.319							
		$^2\Pi$	RCCSD(T)/cc-pVTZ[c]	$C_{\infty v}$	1.065	1.228	1.339	1.273	1.318							
		$^2\Pi$	Expt. - FTM[d]	$C_{\infty v}$	1.055	1.224	1.329	1.267	1.308							
		$^4\Sigma^-$	B3LYP/cc-pVDZ[a]	$C_{\infty v}$	1.072	1.243	1.322	1.298	1.267							
II	Anion	$^1A_1$	B3LYP/cc-pVDZ[a]	C_{2v}	1.070	1.229	1.393	1.407	1.469	180.0	180.0	148.5	58.5			
	Neutral	$^2B_2$	B3LYP/cc-pVDZ[a]	C_{2v}	1.074	1.219	1.384	1.401	1.371	180.0	180.0	150.7	60.7			
		$^2B_2$	EOMIP-CCSD/TZ2P[b]	C_{2v}	1.062	1.204	1.395	1.383	1.363	180.0	180.0	150.4	60.4			
		$^2A_1$	B3LYP/cc-pVDZ[a]	C_{2v}	1.073	1.217	1.393	1.401	1.503	180.0	180.0	147.5	57.5			
III	Anion	$^1A'$	B3LYP/cc-pVDZ[a]	C_s	1.094	1.398	1.479	1.376	1.264	147.3	56.5	150.7	179.5	180.0	180.0	0.0
	Neutral	^2A	B3LYP/cc-pVDZ[a]	C_s	1.088	1.348	1.460	1.328	1.291	155.8	60.5	156.8	179.1	180.0	180.0	180.0
		$^2A'$	EOMIP-CCSD/TZ2P[b]	C_s	1.073	1.336	1.444	1.320	1.275	156.4	61.2	156.2	178.4	180.0	180.0	180.0
IV	Anion	$^1A_1$	B3LYP/cc-pVDZ[a]	C_{2v}	1.271	1.380	1.380	1.271	1.108	176.2	129.0	176.2	115.5	180.0	180.0	0.0
	Neutral	$^2B_2$	B3LYP/cc-pVDZ[a]	C_{2v}	1.293	1.371	1.371	1.293	1.098	176.0	112.2	176.0	123.9	180.0	180.0	0.0
		^2A	EOIMP-CCSD/DZP[b]	C_1	1.308	1.376	1.403	1.296	1.096	171.7	120.1	161.2	119.1	116.7	−120.0	71.0

[a]This work.
[b]Reference 20.
[c]Reference 14.
[d]Reference 23.

tures found by Blanksby *et al.*[27] at a similar level of theory. Table III shows the current B3LYP calculated vibrational frequencies for the anion and neutral states of each isomer. Table IV shows current as well as previous calculated energetics for both the anion and neutral manifolds.

Isomer I of C_5H corresponds to the linear or slightly bent chain form, analogous to the linear isomer of C_3H. According to the B3LYP calculations, the anion has a bent ^3A ground state. The structure converged to a geometry with C_1 symmetry, corresponding to a $^3\Sigma^-$ state at the linear geometry. The $^3\Sigma^-$ electronic configuration is $\cdots(2\pi)^4(11\sigma)^2(3\pi_x)^1(3\pi_y)^1$ which upon bending to the C_1 geometry gives $\cdots(13a)^2(14a)^2(15a)^2(16a)^1(17a)^1$. Ejection of a $(16a)$ or $(17a)$ electron leads to the electronic configuration for the $^2\Pi$ ground state of the neutral $\cdots(2\pi)^4(11\sigma)^2(3\pi)^1$. In the neutral, the B3LYP calculations converge to a strictly linear structure. The acetylenic character of the carbon chain, as evidenced by how much the bond lengths alternate, is comparable to the RCCSD(T) calcula-

TABLE III. Calculated frequencies.

		State	Method	Sym.	ν_1	ν_2	ν_3	ν_4	ν_5	ν_6	ν_7	ν_8	ν_9	ν_{10}	ν_{11}	ν_{12}	ν_{13}
I					σ^+/a	σ^+/a	σ^+/a	σ^+/a	σ^+/a	π_x/a	π_y/a	π_x/a	π_y/a	π_x/a	π_y/a	π_x/a	π_y
	Anion	^3A	B3LYP/cc-pVDZ[a]	C_1	3368	1890	1828	1475	770	609	631	397	160	435	443	162	⋯
	Neutral	$^2\Pi$	B3LYP/cc-pVDZ/TZ2P[a]	$C_{\infty v}$	3462	2064	1970	1466	775	542	683	411	772	395	328	142	146
		$^2\Pi$	EOMEA-CCSD/TZ2P[b]	$C_{\infty v}$	3478	2091	1945	1420	747	526	535	358	715	305	292	64	167
		$^4\Sigma^-$	B3LYP/cc-pVDZ[a]	$C_{\infty v}$	3465	1984	1749	1566	783	491	491	499	499	403	403	149	149
II					a_1	a_1	a_1	a_1	a_1	b_2	b_2	b_2	b_2	b_1	b_1	b_1	
	Anion	$^1A_1$	B3LYP/cc-pVDZ[a]	C_{2v}	3490	2116	1600	979	691	181	527	207	1192	640	598	248	
	Neutral	$^2B_2$	B3LYP/cc-pVDZ[a]	C_{2v}	3464	2163	1657	1286	745	646	536	175	458	743	572	230	
		$^2B_2$	EOMIP-CCSD/TZ2P[b]	C_{2v}	3470	2191	1652	1279	728	722	539	202	365	672	527	132	
		$^2A_1$	B3LYP/cc-pVDZ[a]	C_{2v}	3473	2200	1635	941	677	598	505	204	2223	746	556	230	
III					a'	a'	a'	a'	a'	a'	a'	a'	a'	a''	a''	a''	
	Anion	$^1A'$	B3LYP/cc-pVDZ[a]	C_s	3136	2060	1659	1316	904	1065	701	513	223	844	567	237	
	Neutral	$^2A'$	B3LYP/cc-pVDZ[a]	C_s	3269	2020	1636	1289	969	842	731	450	172	823	541	194	
		$^2A'$	EOMIP-CCSD/TZ2P[b]	C_s	3316	2024	1632	1288	1000	851	736	449	151	822	511	139	
IV					a_1/a	a_1/a	a_1/a	a_1/a	a_1/a	b_2/a	b_2/a	b_2/a	b_2/a	b_1/a	b_1/a	a_2/a	
	Anion	$^1A_1$	B3LYP/cc-pVDZ[a]	C_{2v}	2987	2060	962	580	155	2035	1398	1170	323	902	286	309	
	Neutral	$^2B_2$	B3LYP/cc-pVDZ[a]	C_{2v}	3133	1924	1043	510	97	1778	1295	1040	200	757	243	271	
		^2A	EOIMP-CCSD/DZP[b]	C_1	3198	1877	993	407	90	1466	1312	947	191	870	241	110	

[a]This work.
[b]Reference 16.

TABLE IV. Calculated relative energetics for the anion and neutral manifolds. The numbers in parentheses are zero-point corrected. Numbers in square brackets are calculated detachment energies between the zero-point levels of the corresponding anion and neutral electronic states. The zero of the energy scales for both manifolds are taken from isomer I.

		Isomer I		Isomer II		Isomer III	Isomer IV
Anion		^3A		$^1A_1$		$^1A'$	$^1A_1$
	B3LYP/cc-pVDZ[a]	0.000 (0.000)		0.688 (0.707)		0.285(0.351)	0.173(0.235)
	RCCSD(T)/aug-cc-pVDZ[b]	0.000 (0.000)		0.088 (0.133)		−0.206(−0.114)	−0.239(−0.150)
Neutral		$^2\Pi$	$^4\Sigma^-$	$^2B_2$	$^2A_1$	$^2A'$	$^2B_2$ (^2A)[d]
	B3LYP/cc-pVDZ[a]	0.000(0.000)[2.209]	1.358(1.325)	0.472(0.443)[1.944]	1.420(1.472)	0.980(0.967)[2.825]	2.235(2.182)[4.155]
	RCCSD(T)/aug-cc-pVDZ[b]	0.000(0.000)[2.321]		0.147(0.199)[2.388]		0.845(0.906)[3.344]	2.026(2.063)[4.538]
	CCSD(T)/DZP[c]	0.000(0.000)		0.212(0.273)		0.954(0.975)	2.155(2.129)[d]

[a]This work.
[b]Reference 27.
[c]Reference 16.
[d]Estimated from EOMIP-CCSD*/DZP calculations of Ref. 16 which converged to lower symmetry C_1 structure.

tions by Woon[15] but is less than in the EOMEA-CCSD study.[16] The B3LYP bond lengths differ by about 0.01 Å from the microwave data[19] except for the CH bond length, which is longer by about 0.02 Å. The lower bond length obtained from experimental rotational constants is presumably due to vibrational averaging over the large amplitude CCH bend, as was the case in C_3H.[45]

The $^2\Pi$ electronic state is susceptible the Renner–Teller effect, the interaction of electronic and vibrational angular momentum in a linear molecule, which serves to split the energies of the normally degenerate bending modes. Calculated vibrational frequencies for the bending modes of C_5H show splittings suggestive of these effects. The largest splitting of 360 cm^{-1} occurs for ν_8/ν_9, the predominantly CCH bending mode, but these effects also appear in the three C—C—C bending modes. Splittings are also seen for the higher level EOMEA-CCSD calculations of Crawford *et al.*[16]

Detachment of a $(15a)$ electron from the ^3A anion state (isomer I) leads to the electronic configuration $\cdots(2\pi)^4(11\sigma)^1(3\pi_x)^1(3\pi_y)^1$, a linear quartet $^4\Sigma^-$ excited state calculated to lie 1.357 eV above the $^2\Pi$ state. This state lies considerably below any of the doublet excited states calculated by Haubrich *et al.*[17] Unlike the ground state, the quartet state does not suffer from symmetry-breaking effects in the bending modes. C_3H also has a $^4\Sigma^-$ excited state to which detachment transitions were observed.[26]

Isomer II is a ring-chain structure with the hydrogen at the end of the chain, and is referred to henceforth as either isomer II or the cyclic isomer. An analogy can be made between its anion and neutral electronic states and those of the cyclic isomer of C_3H. The anion ($^1A_1$) is closed shell with C_{2v} symmetry and a $\cdots(3b_2)^2(2b_1)^2(10a_1)^2(4b_2)^2$ electronic configuration. Two electronic states of the neutral were calculated. Removal of an outer $(4b_2)$ electron leads to the $\cdots(3b_2)^2(2b_1)^2(10a_1)^2(4b_2)^1$ electronic configuration of the $^2B_2$ state, and removal of a $(10a_1)$ electron leads to the $^2A_1$ state $[\cdots(3b_2)^2(2b_1)^2(10a_1)^1(4b_2)^2]$, lying 0.948 eV higher. This value is close to but slightly lower than the previously reported vertical excitation energy of 1.27 eV.[17] The EOMIP-CCSD calculations[16] also converge to a symmetric C_{2v} structure. However, just as for C_3H, the $^2B_2$ state of C_5H is expected to undergo a pseudo-Jahn–Teller interaction with the $^2A_1$ excited state which may distort the equilibrium geometry to lower symmetry.[46] Fourier-transform microwave spectroscopy on C_5H indicates a slightly distorted C_3 ring based on the observation of the nominally forbidden $K=0$ rotational ladder.[29]

Isomer III is also a derivative of the cyclic C_3H isomer, yet the electronic structure is very different. The C_s structure gives rise to a $\cdots(12a')^2(2a'')^2(13a')^2(14a')^2$ electronic configuration of a $^1A'$ electronic state. Detachment of the outermost electron leads to a $^2A'$ state. The calculated B3LYP neutral structure is very similar to that of the EOMIP-CCSD calculations.[47] The frequencies at the B3LYP level also compare very favorably to the higher level calculations, with the largest discrepancy being only 55 cm^{-1} in the lowest frequency mode.

Isomer IV is unique in that it is a bent chain with the hydrogen at the center carbon, whereas most structures find the hydrogen at the end of the chain or on a ring. The anion calculation converges to a symmetric C_{2v} structure ($^1A_1$) with an electron configuration of $\cdots(5b_2)^2(1a_2)^2(8a_1)^2(6b_2)^2$. Photodetachment from the $(6b_2)$ orbital leads to the lowest energy $^2B_2$ neutral state. The B3LYP calculations on the neutral converge to the more symmetric C_{2v} structure, while the higher level EOMIP-CCSD calculations of Crawford *et al.*[16] find an asymmetric ^2A (C_1) state to be the minimum. Despite this fact, the calculated frequencies show reasonable agreement. The majority of the frequencies agree within $\sim$100 cm^{-1} with the notable exception of ν_6, an asymmetric carbon stretching mode.

Table IV gives the energies of the electronic states for the four isomers calculated in the current and previous works. Relative energies are given within both the anion and neutral manifolds. Numbers in parentheses include zero-point corrections. Numbers in square brackets are calculated adiabatic detachment energies between anion and neutrals of the same isomer. Within the anion and neutral manifolds, the energy of the linear isomer is set to zero. The B3LYP calculations find the linear/bent isomer to be the ground state for both the anion and neutral. In the anion, isomer IV is less stable than the linear isomer by 0.173 eV. Isomers III and II

are 0.285 and 0.688 eV higher in energy, respectively. At the RCCSD(T) level of theory, the linear isomer is destabilized relative to isomer IV, while isomers II and III are more stable in comparison. On the neutral potential energy surface, the $^2\Pi$ state of the linear isomer is universally the ground state, with isomers II, III, and IV progressively higher in energy.

IV. DISCUSSION

A. General considerations

The spectra at 355 nm resemble a vibrational intensity pattern arising from a single electronic transition. However, close-lying electronic transitions from different isomers could also produce the same effect. C_3H^-, in particular, demonstrated the possibility of such isomers, showing overlapped photodetachment transitions from linear and cyclic forms with similar *e*BEs.[26] With a larger molecule such as C_5H^-, in which many more stable isomeric forms are predicted, this possibility is even more likely. In C_3H^-, we were able to distinguish photodetachment transitions originating from the linear and cyclic isomers by means of the photoelectron angular distributions and variations in relative peak intensities depending on whether propyne or acetylene was used as the starting material. Preliminary data on C_5H^- produced with acetylene were inconclusive as to whether or not real intensity variations due to the formation of different isomers were present. In regards to angular distributions, the anisotropy parameter for A_0 in the C_5H^- spectrum at both 299 and 266 nm is slightly less than that for X_0 and X_1 (−0.1 vs −0.2, see Table I). The significance of this difference is unclear given that A_0 sits on top of significant underlying signal, complicating the accurate determination of its intensity. However, as mentioned in Sec. III A, the greatly increased relative intensity of peak A_0 at 299 and 266 nm compared to 355 nm does suggest it arises from a different electronic transition or isomer than band *X*.

Of the four isomers depicted in Fig. 2, only isomers I and II are predicted to have detachment energies in the range of *e*BEs reported for bands *X* and A_0 (see Table IV). The detachment energies from Blanksby *et al.*[27] for the $^2\Pi \leftarrow {}^3A$ (isomer I, 2.321 eV) and $^2B_2 \leftarrow {}^1A_1$ (isomer II, 2.388 eV) transitions show a good agreement with the *e*BE of X_0 (2.421 eV). In fact, the analysis presented in the next section strongly supports assigning band *X* to isomer I, in which case A_0 would most likely be from isomer II. For the higher energy bands, B_0 at 3.720 and *C* at ~3.8–3.9 eV, possible candidates include transitions from anion isomers III and IV to the corresponding neutral ground states, and transitions from anion isomers I and II to the low-lying neutral linear $^4\Sigma^-$ and cyclic $^2A_1$ excited states, as calculated in Sec. III B. Assignments of bands *B* and *C* are considered further in the following section once the origin of band *X* is established.

B. Franck–Condon simulations: Band *X*

In the assignment of band *X*, the first point to consider is that peaks X_0, X_1, and X_2 are spaced by 1964 cm^{-1}, on average, which is in good agreement with the calculated frequencies for the totally symmetric ν_3 mode of the neutral $^2\Pi$ state (see Table III). In contrast, the closest calculated frequencies for the $^2B_2$ cyclic state are either 200 cm^{-1} above or 300 cm^{-1} below this spacing. In addition, the 355 nm spectra are unusually congested, showing a small number of peaks superimposed on what appears to be a dense manifold of partially resolved features. The overall appearance of this band suggests a large number of active, low frequency modes. The neutral $^2\Pi$ state has several low frequency bending modes, many of which will be active in the $^2\Pi \leftarrow {}^3A$ transition due to the difference in symmetry between the anion and neutral. For these reasons, the $^2\Pi \leftarrow {}^3A$ transition of the linear isomer is an excellent candidate for band *X*. We test both this assignment and the possibility that band *X* arises from the $^2B_2 \leftarrow {}^1A_1$ transition of the cyclic isomer via FC simulations used in conjunction with our electronic structure calculations.

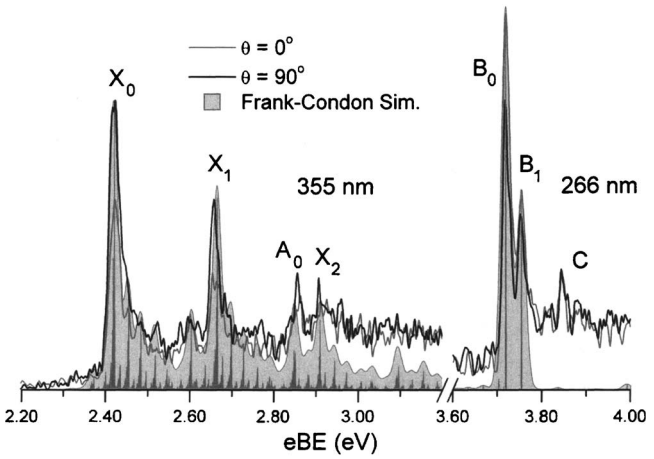

FIG. 3. Franck–Condon (FC) simulations of bands *X* and *B* in the 355 and 266 nm spectra.

The simulations were carried out treating each mode as an independent harmonic oscillator under the parallel mode approximation. The FCFGAUS program of Ervin *et al.*[48] was used to extract the normal coordinate displacement vectors from the GAUSIAN03 output. These values as well as the vibrational temperature (300 K was used for all simulations), the anion and neutral vibrational frequencies, and a Gaussian peak width were used as input into the PESCAL program.[49] The program calculates FC factors and transition energies for the stick spectra and convolutes them with Gaussian functions to obtain the simulated spectrum. Figure 3 shows the best-fit FC simulations of bands *X* and *B* overlapped with the appropriate spectra. Band *X* was simulated using the 355 nm data, while band *B* was simulated using the 266 nm data. Gaussian peak widths of 25 meV were used in both the *X* and *B* simulation. No account was taken in the simulation for the variation in peak width with *e*KE, as described in Sec. II.

To reproduce band *X*, simulations were undertaken for the two transitions discussed in the previous section: $^2\Pi \leftarrow {}^3A$ (isomer I) and $^2B_2 \leftarrow {}^1A_1$ (isomer II). In each case, the B3LYP frequencies and geometries were used as a starting point. For the $^2B_2 \leftarrow {}^1A_1$ simulation, the dominant active modes are the ν_4 ring scissoring motion at 1286 cm^{-1}, followed by the ν_3 symmetric ring stretch at 1657 cm^{-1}. All other modes show much less activity and contribute little intensity to the simulation. The simulation is not shown but it

is immediately clear that the active frequencies are off by 626 and 255 cm^{-1}, respectively, from the X_0-X_1 spacing of 1912 cm^{-1}. Although the FC factors for the 1286 cm^{-1} mode are approximately correct for the X_0-X_1-X_2 series, the frequency discrepancy is large enough to rule out the cyclic isomer as a possibility for band *X*.

Now we discuss the $^2\Pi \leftarrow {}^3A$ simulation. Upon photodetachment from the ^3A (C_1) state of the linear anion to the $^2\Pi$ neutral state with $C_{\infty v}$ symmetry, all five stretching modes and all eight bending modes of the neutral are nominally active (each degenerate mode is counted as two, based on the lower overall symmetry of the problem). The simulation obtained from the calculations with no adjustment predicts significant activity in the 411 cm^{-1} CCH bend (ν_8), the 395 cm^{-1} CCC bend (ν_{10}), and the 1970 cm^{-1} asymmetric stretch (ν_3). The optimized simulation, shown in Fig. 3, was obtained by increasing ΔQ_3, the normal coordinate displacement of mode 3 between the anion and neutral, to gain more activity in the $\Delta\nu_3$ mode, while reducing Q_8 to decrease activity in the CCH bending mode. In addition, small adjustments to displacements and frequencies were applied to reproduce the shape of the partially resolved signal underlying the main peaks.

Fixing the neutral geometry at the calculated values, the optimized anion geometry has bond lengths $r_a - r_e$ of 1.074, 1.264, 1.289, 1.325, and 1.244 Å, respectively (see Fig. 2) and CCH bond angle $\alpha_e = 161.2°$. Comparison to the calculated anion structure in Table II shows that the changes in bond length are quite small, and that the largest discrepancy is in α_e, which is 150.5° in Table II. It is perhaps not too surprising that the CCH bending mode is problematic from the perspective of our one-dimensional harmonic analysis, given that the CCH bend is a large-amplitude motion likely to experience strong Renner–Teller splitting, as was the case for the analogous mode in linear C_3H.[50] In any case, based on this simulation, band *X* is assigned as the $^2\Pi \leftarrow {}^3A$ transition of the linear isomer with X_0 as the origin giving an *e*BE of 2.421 ± 0.019 eV. X_1 corresponds to the 3_0^1 transition giving a frequency of 1912 ± 40 cm^{-1} for the ν_3 antisymmetric stretching mode. X_2 corresponds to the 3_0^2 overtone. With the assignment of band *X*, the assignment of other bands is greatly facilitated.

C. Assignment of other bands

Peak A_0 lies 0.434 eV (3516 cm^{-1}) from X_0, close to the calculated frequency of the ν_1 C—H stretch of the neutral $^2\Pi$ state. In the absence of the 299 and 266 nm data, we would assign it to the 1_0^1 vibrational transition, and this transition may, indeed, contribute some intensities to peak A_0 at 355 nm. However, in light of our assignment of band *X*, peak A_0 is either a transition from the ^3A anion to a low-lying linear excited state of isomer I or a transition involving different structural isomers. Our calculations (Sec. III B) predict the lowest linear excited state ($^4\Sigma^-$) to lie 1.325 eV above the $^2\Pi$ state, which is significantly higher than the X_0-A_0 splitting. Therefore, we assign A_0 as the $^2B_2 \leftarrow {}^1A_1$ transition of isomer II. The detachment energy of isomer II implied by this assignment, 2.857 ± 0.028 eV, is somewhat higher than the detachment energy calculated by Blanksby *et al.*,[27] 2.388 eV, but our assignment appears to be the most plausible option based on the considerations given in Sec. IV A.

We now discuss the assignment of band *B*. Energetically (see Table IV), there are four unassigned transitions accessible at both 299 and 266 nm that are candidates for this band: $^4\Sigma^- \leftarrow {}^3A$ (isomer I), $^2A_1 \leftarrow {}^1A_1$ (isomer II), $^2A' \leftarrow {}^1A'$ (isomer III), and $^2B_2 \leftarrow {}^1A_1$ (isomer IV). Three supporting pieces of evidence serve to narrow the choices and to identify band *B* as the $^2A_1 \leftarrow {}^1A_1$ transition of the cyclic isomer. First of all, with the assignment of bands *X* and *A* to the linear and cyclic isomers, we expect to see transitions to their excited states. Second, assignments of bands *X* and *A* give better estimates for the excited state detachment energies. The $^4\Sigma^-$ state is calculated to lie 1.325 eV above X_0, giving a detachment energy of 3.746 eV, while the $^2A_1$ cyclic state is calculated to lie 1.029 eV above A_0, giving 3.886 eV. Both of these values are in excellent agreement with the *e*BE of B_0 (3.720 eV). Third, confirmation of the assignment is given with the FC simulation, as described below.

Band *B* was simulated most readily using the calculated cyclic $^2A_1 \leftarrow {}^1A_1$ transition; the optimized simulation is shown in Fig. 3. Pure calculated simulations of the $^2A' \leftarrow {}^1A'$ transition of isomer III, the $^2B_2 \leftarrow {}^1A_1$ transition of isomer IV, and the linear excited state transition, $^4\Sigma^- \leftarrow {}^3A$, showed much more extended vibrational progressions due to larger geometry changes. From the simulation in Fig. 3, B_0 corresponds to the origin with an *e*BE of 3.720 ± 0.012 eV. B_1 is assigned as 5_0^1, the symmetric ring scissor mode with a frequency of 282 ± 40 cm^{-1}. Peaks A_0 and B_0 are separated by 0.863 eV, which is close to the calculated $^2A_1$ term energy of 1.029 eV. Hence, the assignment of band *B* is not only reasonable based on its vibrational structure but is also also consistent with our assignment of peak A_0 given above.

The assignment of band *C* warrants similar considerations as for band *B*. The $^4\Sigma^- \leftarrow {}^3A$ transition is the most likely based on assignment of X_0 to the $^2\Pi$ state and the estimated detachment energy (3.746 eV). However, the low intensity and noisy background around band *C* did not allow for proper FC analysis. In any case, a qualitative comparison is still useful. Like the bent to linear transition of the ground state, the $^4\Sigma^- \leftarrow {}^3A$ transition shows significant activity in the CCH bend ($\nu_8/\nu_9 = 499$ cm^{-1}) as well as moderate activity in the other low frequency bending modes. Additionally, like the 355 nm spectrum around band *X*, the 299 and 266 nm data in the region of *C* show considerable noise. In conjunction, this evidence suggests a scenario identical to the hypothesis for band *X*; a transition involving multiple, low frequency active modes contributing to a broad, unresolvable signal with faint structure superimposed thereupon. Therefore, *C* is assigned as the transition from the anion to the first excited linear quartet state: $^4\Sigma^- \leftarrow {}^3A$. A precise determination of the origin is not feasible due to the considerations discussed above, although the detachment energy is approximately 3.80 eV.

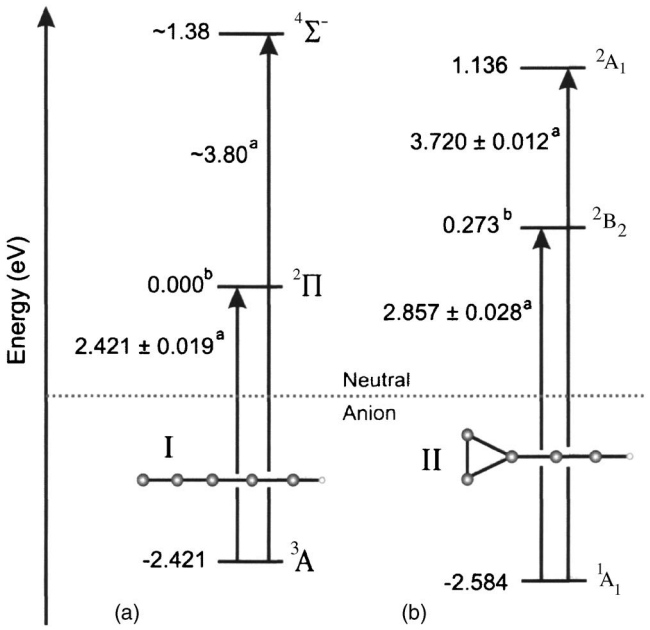

FIG. 4. Energy level diagram of isomers I and II based on the experimental detachment energies (a) and the CCSD(T) calculations of Ref. 16 (b). Energies are relative to the $^2\Pi$ neutral ground state of the linear isomer.

Figure 4 shows a schematic of the relative energetics of the C_5H isomers using current experimental numbers and available calculations. Only isomers I and II are shown since we have not assigned any observed bands to the other isomers. The relative energies of the $^2\Pi$ and $^2B_2$ neutral states are fixed by the values calculated at the CCSD(T) level of theory by Crawford *et al.*[16] The energy of the excited state of the cyclic isomer ($^2A_1$) is determined from the A_0-B_0 splitting (0.863 eV) to be 1.136 eV above the $^2\Pi$ ground state. The $^4\Sigma^-$ state is estimated to be 1.38 eV above the $^2\Pi$ ground state from the approximate *e*BE of band *C*. From the experimental detachment energies for the linear (X_0, 2.421 eV) and cyclic (A_0, 2.857 eV) the relative energies of the anion isomers I and II are determined. Using this scheme, in which we assume the calculated neutral energetics by Crawford *et al.* to be correct, the cyclic $^1A_1$ state is found to be 0.163 eV lower in energy than the linear ^3A anion.

V. CONCLUSIONS

We have identified detachment transitions arising from two isomers of the C_5H anion in the photoelectron spectra. Analogous to the transitions observed in C_3H^-, this work presents evidence that both a linear and cyclic isomers of C_5H^- lie very close in energy to one another, with the cyclic form as the lower state. Peaks arising from different isomers were assigned on the basis of Franck–Condon simulations and intensity variations with detachment energy.

ACKNOWLEDGMENTS

This research is supported by the National Science Foundation under Grant No. DMR-0139064.

[1] X. Gu, Y. Guo, and R. I. Kaiser, Int. J. Mass. Spectrom. **261**, 100 (2007).
[2] D. C. Clary, E. Buonomo, I. R. Sims, I. W. M. Smith, W. D. Geppert, C. Naulin, M. Costes, L. Cartechini, and P. Casavecchia, J. Phys. Chem. A **106**, 5541 (2002).
[3] A. M. Mebel, G. S. Kim, V. V. Kislov, and R. I. Kaiser, J. Phys. Chem. A **111**, 6704 (2007).
[4] T. G. Phillips and P. J. Huggins, Astrophys. J. **251**, 533 (1981).
[5] J. Zmuidzinas, A. L. Betz, R. T. Boreiko, and D. M. Goldhaber, Astrophys. J. **335**, 774 (1988).
[6] N. J. Evans, J. H. Lacy, and J. S. Carr, Astrophys. J. **383**, 674 (1991).
[7] P. F. Bernath, K. H. Hinkle, and J. J. Keady, Science **244**, 562 (1989).
[8] J. Cernicharo and M. Guelin, Astron. Astrophys. **309**, L27 (1996).
[9] J. Cernicharo, M. Guelin, M. Agundez, K. Kawaguchi, M. C. McCarthy, and P. Thaddeus, Astron. Astrophys. **467**, L37 (2007).
[10] M. C. McCarthy, C. A. Gottlieb, H. Gupta, and P. Thaddeus, Astrophys. J. **652**, L141 (2006).
[11] S. Brunken, H. Gupta, C. A. Gottlieb, M. C. McCarthy, and P. Thaddeus, Astrophys. J. **664**, L43 (2007).
[12] C. A. Gottlieb, E. W. Gottlieb, and P. Thaddeus, Astron. Astrophys. **164**, L5 (1986).
[13] J. Cernicharo, C. Kahane, J. Gomezgonzalez, and M. Guelin, Astron. Astrophys. **167**, L5 (1986).
[14] D. L. Cooper and S. C. Murphy, Astrophys. J. **333**, 482 (1988).
[15] D. E. Woon, Chem. Phys. Lett. **244**, 45 (1995).
[16] T. D. Crawford, J. F. Stanton, J. C. Saeh, and H. F. Schaefer, J. Am. Chem. Soc. **121**, 1902 (1999).
[17] J. Haubrich, M. Muhlhauser, and S. D. Peyerimhoff, J. Phys. Chem. A **106**, 8201 (2002).
[18] L. Pan, B. K. Rao, A. K. Gupta, G. P. Das, and P. Ayyub, J. Chem. Phys. **119**, 7705 (2003).
[19] M. C. McCarthy and P. Thaddeus, J. Chem. Phys. **122**, 174308 (2005).
[20] H. Ding, T. Pino, F. Guthe, and J. P. Maier, J. Chem. Phys. **117**, 8362 (2002).
[21] C. A. Gottlieb, J. M. Vrtilek, E. W. Gottlieb, P. Thaddeus, and A. Hjalmarson, Astrophys. J. **294**, L55 (1985).
[22] S. Yamamoto, S. Saito, M. Ohishi, H. Suzuki, S. Ishikawa, N. Kaifu, and A. Murakami, Astrophys. J. **322**, L55 (1987).
[23] S. Yamamoto, S. Saito, H. Suzuki, S. Deguchi, N. Kaifu, S. I. Ishikawa, and M. Ohishi, Astrophys. J. **348**, 363 (1990).
[24] S. Yamamoto and S. Saito, Astrophys. J. **363**, L13 (1990).
[25] J. M. Oakes and G. B. Ellison, Tetrahedron **42**, 6263 (1986).
[26] S. M. Sheehan, B. F. Parsons, J. Zhou, E. Garand, T. Yen, D. T. Moore, and D. M. Neumark, J. Chem. Phys. **128**, 034301 (2008).
[27] S. J. Blanksby, S. Dua, and J. H. Bowie, J. Phys. Chem. A **103**, 5161 (1999).
[28] S. J. Blanksby, S. Dua, J. H. Bowie, and J. C. Sheldon, Chem. Commun. (Cambridge) **1997**, 1833.
[29] A. J. Apponi, M. E. Sanz, C. A. Gottlieb, M. C. McCarthy, and P. Thaddeus, Astrophys. J. **547**, L65 (2001).
[30] C. A. Gottlieb, E. W. Gottlieb, P. Thaddeus, and H. Kawamura, Astrophys. J. **275**, 916 (1983).
[31] K. Hoshina, H. Kohguchi, Y. Ohshima, and Y. Endo, J. Chem. Phys. **108**, 3465 (1998).
[32] H. Linnartz, T. Motylewski, O. Vaizert, J. P. Maier, A. J. Apponi, M. C. McCarthy, C. A. Gottlieb, and P. Thaddeus, J. Mol. Spectrosc. **197**, 1 (1999).
[33] T. R. Taylor, C. S. Xu, and D. M. Neumark, J. Chem. Phys. **108**, 10018 (1998).
[34] J. Zhou, E. Garand, and D. M. Neumark, J. Chem. Phys. **127**, 154320 (2007).
[35] S. Dua, J. C. Sheldon, and J. H. Bowie, J. Chem. Soc., Chem. Commun. **1995**, 1067.
[36] J. Zhou, E. Garand, and D. M. Neumark, J. Chem. Phys. **127**, 114313 (2007).
[37] C. Xu, G. R. Burton, T. R. Taylor, and D. M. Neumark, J. Chem. Phys. **107**, 3248 (1997).
[38] R. B. Metz, A. Weaver, S. E. Bradforth, T. N. Kitsopoulos, and D. M. Neumark, J. Phys. Chem. **94**, 1377 (1990).
[39] G. Markovich, R. Giniger, M. Levin, and O. Cheshnovsky, J. Chem. Phys. **95**, 9416 (1991).
[40] J. Cooper and R. N. Zare, J. Chem. Phys. **48**, 942 (1968).
[41] C. T. Lee, W. T. Yang, and R. G. Parr, Phys. Rev. B **37**, 785 (1988).
[42] A. D. Becke, J. Chem. Phys. **98**, 1372 (1993).

[43] T. H. Dunning, J. Chem. Phys. **90**, 1007 (1989).
[44] M. J. Frisch, G. W. Trucks, H. B. Schlegel *et al.*, GAUSSIAN 03, Revision C.02 Gaussian, Inc., Wallingford, CT, 2004.
[45] M. Kanada, S. Yamamoto, S. Saito, and Y. Osamura, J. Chem. Phys. **104**, 2192 (1996).
[46] J. F. Stanton, Chem. Phys. Lett. **237**, 20 (1995).
[47] P. Thaddeus, M. Guelin, and R. A. Linke, Astrophys. J. **246**, L41 (1981).
[48] K. M. Ervin, T. M. Ramond, G. E. Davico, R. L. Schwartz, S. M. Casey, and W. C. Lineberger, J. Phys. Chem. A **105**, 10822 (2001).
[49] K. M. Ervin, Fortran PESCAL, 2001.
[50] M. Peric, M. Mladenovic, K. Tomic, and C. M. Marian, J. Chem. Phys. **118**, 4444 (2003).